

Radial-orbit instability in modified Newtonian dynamics

Carlo Nipoti,^{1*} Luca Ciotti¹ and Pasquale Londrillo²

¹*Astronomy Department, University of Bologna, via Ranzani 1, I-40127 Bologna, Italy*

²*INAF-Bologna Astronomical Observatory, via Ranzani 1, I-40127 Bologna, Italy*

Accepted 2011 March 2. Received 2011 February 28; in original form 2011 January 31

ABSTRACT

The stability of radially anisotropic spherical stellar systems in modified Newtonian dynamics (MOND) is explored by means of numerical simulations performed with the N -body code *N-MODY*. We find that Osipkov-Merritt MOND models require for stability larger minimum anisotropy radius than equivalent Newtonian systems (ENSs) with dark matter, and also than purely baryonic Newtonian models with the same density profile. The maximum value for stability of the Fridman-Polyachenko-Shukhman parameter in MOND models is lower than in ENSs, but higher than in Newtonian models with no dark matter. We conclude that MOND systems are substantially more prone to radial-orbit instability than ENSs with dark matter, while they are able to support a larger amount of kinetic energy stored in radial orbits than purely baryonic Newtonian systems. An explanation of these results is attempted, and their relevance to the MOND interpretation of the observed kinematics of globular clusters, dwarf spheroidal and elliptical galaxies is briefly discussed.

Key words: dark matter — galaxies: kinematics and dynamics — globular clusters: general — gravitation — instabilities

1 INTRODUCTION

Modified Newtonian dynamics (MOND) was originally proposed by Milgrom (1983) to explain the rotation curves of disk galaxies without invoking the presence of dark matter (DM) and, over the years, it has been successful at reproducing the observed kinematics of several galaxies (e.g. Sanders & McGaugh 2002; Sanders & Noordermeer 2007; Swaters, Sanders, & McGaugh 2010, and references therein). However, to some extent, the MOND and DM interpretations of the kinematics of galaxies can be degenerate. For instance, a MOND rotation curve can be also described in the Newtonian gravity invoking a DM halo such that the total gravitational field is the same as the MOND one. More generally, given a MOND system, it is possible to construct the *equivalent Newtonian system* (ENS), i.e. the Newtonian system with DM in which the visible matter has the same phase-space distribution as in the MOND system (Milgrom 1986, 2001; Nipoti et al. 2007b; Nipoti, Londrillo & Ciotti 2007c; Nipoti et al. 2008). It should be noted, however, that the physical viability of the ENS is not guaranteed, as for some configurations the density of the associate DM halo turns out to be negative (Milgrom 1986). Though a MOND system and its ENS are, by construction, indistinguishable from a *kinematic* point of view (for instance, as far as the rota-

tion curve¹ or the velocity-dispersion profile are concerned), in general they are not identical from a *dynamical* point of view: for instance, two-body relaxation, dynamical friction and galaxy merging act differently in the two cases (Ciotti & Binney 2004; Nipoti et al. 2007c, 2008).

As already recognized, MOND and ENSs might differ substantially also in terms of stability. As one of the original motivations for invoking DM halos in disk galaxies was that purely baryonic Newtonian disks are prone to bar-like instability (Ostriker & Peebles 1973), it is not surprising that the study of dynamical stability in MOND has focused mainly on disks (Milgrom 1989; Christodoulou 1991; Brada & Milgrom 1999). Here we consider instead the so-called radial-orbit instability, which is relevant to pressure-supported stellar systems. As well known, in the context of Newtonian gravity the amount of radial orbits in stellar systems is limited not only by the requirement of phase-space consistency (i.e. positivity of the distribution function; see, e.g., Ciotti & Pellegrini 1992; An & Evans 2006; Ciotti & Morganti 2009, 2010a,b) but also by the fact that very radially anisotropic spherical systems are unstable (Henon 1973; Polyachenko & Shukhman 1981; Fridman & Polyachenko 1984; Merritt &

¹ The MOND rotation curve of a disk galaxy can be always reproduced with a *spherical* DM halo and Newtonian gravity. However, the vertical kinematics differs in the two cases (Nipoti et al. 2007b), because the DM halo of the ENS of a disk galaxy is non-spherical.

* E-mail: carlo.nipoti@unibo.it

Aguilar 1985; Barnes, Hut, & Goodman 1986; May & Binney 1986; Palmer & Papaloizou 1987; Dejonghe & Merritt 1988; Saha 1991; Weinberg 1991; Bertin et al. 1994; Hjorth 1994; Meza & Zamorano 1997; Trenti & Bertin 2006; Barnes, Lanzel, & Williams 2009). In Newtonian gravity DM halos tend to have a stabilizing effect against radial-orbit instability (Stiavelli & Sparke 1991; Meza & Zamorano 1998; Nipoti, Londrillo, & Ciotti 2002), which suggests that MOND systems might be more prone to this kind of instability than their ENSs. If confirmed, this could provide a discriminant between the two theories when interpreting the velocity dispersion profiles in pressure-supported stellar systems. For these reasons, in this work we use N -body simulations to explore the stability of radially anisotropic MOND spherical systems and, for comparison, of their ENSs and of purely baryonic Newtonian systems with the same density distributions and anisotropy profiles.

The paper is organized as follows. In Section 2 the galaxy models used in the simulations are described. Their phase-space consistency is discussed in Section 2.1 and their stability in Section 3. Section 4 concludes.

2 GALAXY MODELS

We consider MOND as modified gravity in the non-relativistic formulation² of Bekenstein & Milgrom (1984), in which the Poisson equation $\nabla^2\phi^N = 4\pi G\rho$ is replaced by

$$\nabla \cdot \left[\mu \left(\frac{\|\nabla\phi\|}{a_0} \right) \nabla\phi \right] = 4\pi G\rho, \quad (1)$$

where $\|\dots\|$ is the standard Euclidean norm, ϕ is the MOND gravitational potential, $a_0 \simeq 1.2 \times 10^{-10} \text{ m s}^{-2}$ is a characteristic acceleration, and μ is the so-called interpolating function (in the present work we adopt $\mu(y) = y/\sqrt{1+y^2}$; Milgrom 1983). The MOND gravitational acceleration is $\mathbf{g} = -\nabla\phi$, just as the Newtonian acceleration is $\mathbf{g}^N = -\nabla\phi^N$. For a system of finite mass, $\nabla\phi \rightarrow 0$ as $\|\mathbf{x}\| \rightarrow \infty$, where \mathbf{x} is the position vector.

As well known, from the Poisson equation and equation (1) it follows that the MOND and Newtonian gravitational accelerations are related by $\mu(g/a_0)\mathbf{g} = \mathbf{g}^N + \mathbf{S}$, where $g \equiv \|\mathbf{g}\|$, and \mathbf{S} is a solenoidal field dependent on the specific ρ considered. Since in general $\mathbf{S} \neq 0$, and its expression is unknown *a priori*, standard Poisson solvers cannot be used to develop MOND N -body codes, in which equation (1) must be solved at each time step (see Brada & Milgrom 1999; Ciotti, Londrillo & Nipoti 2006; Tiret & Combes 2007). In the present work we use our original MOND N -body code N-MODY (Nipoti, Londrillo & Ciotti 2007a; Londrillo & Nipoti 2009, see Section 3.1).

The initial conditions of the simulations are N -body realizations of galaxy models with the stellar component described by a spherical γ -model (Dehnen 1993; Tremaine et al. 1994) with density distribution

$$\rho_*(r) = \frac{3-\gamma}{4\pi} \frac{M_* r_*}{r^\gamma (r_* + r)^{4-\gamma}}, \quad (2)$$

where M_* is the total stellar mass, r_* is the scale radius, and γ is the negative of the inner logarithmic density slope ($0 \leq \gamma < 3$). For simplicity we restrict to the cases $\gamma = 0$ and $\gamma = 1$ (Hernquist 1990); we recall that for $\gamma \neq 2$ the Newtonian potential is

$$\phi_*^N(r) = \frac{GM_*}{r_*(2-\gamma)} \left[\left(\frac{r}{r_* + r} \right)^{2-\gamma} - 1 \right]. \quad (3)$$

For these models the MOND potential, required to distribute the particles in the velocity space, is easily calculated from the Newtonian one, as in spherical symmetry $\mathbf{S} = 0$. The ENS associated with a model of stellar density ρ_* and MOND potential ϕ has a *total* density $\nabla^2\phi(r)/4\pi G$. However, the resulting DM halo density (obtained after subtraction of ρ_*) in principle may be negative or have a non-monotonic radial trend. Fortunately, it can be proved that the DM halos of the ENS derived from the spherical $\gamma = 0$ and $\gamma = 1$ models are everywhere positive. Instead, possible non-monotonicity of the DM density distribution makes the consistency of the halo a non-trivial request, as we will discuss in Section 2.1 (see also Ciotti, Morganti, & de Zeeuw 2009).

In order to impose a tunable amount of radial anisotropy on the initial conditions, we adopt the widely used Osipkov-Merritt (OM) parametrization (Osipkov 1979; Merritt 1985), in which the stellar distribution function depends on energy and angular momentum per unit mass through the variable $Q \equiv \mathcal{E} - J^2/2r_a^2$, where $\mathcal{E} = \Psi - v^2/2$ is the relative energy, $v = \|\mathbf{v}\|$ is the velocity modulus, $\Psi = -\phi$ is the relative potential, J is the angular momentum modulus per unit mass, and r_a is the so-called anisotropy radius. The anisotropy parameter (e.g. Binney & Tremaine 2008) is $\beta(r) = r^2/(r_a^2 + r^2)$: for $r \gg r_a$ the velocity dispersion tensor is radially anisotropic, while for $r \ll r_a$ the tensor is nearly isotropic. In the limit $r_a \rightarrow \infty$, $Q = \mathcal{E}$ and the velocity dispersion tensor becomes globally isotropic.

In the purely baryonic Newtonian models, the distribution function can be written as

$$f_N(Q) = \frac{1}{\sqrt{8\pi^2}} \frac{d}{dQ} \int_0^Q \frac{d\rho_*}{d\Psi_*^N} \frac{d\Psi_*^N}{\sqrt{Q - \Psi_*^N}}, \quad (4)$$

where $\Psi_*^N = -\phi_*^N$ is the Newtonian relative potential and

$$\rho_*(r) = \left(1 + \frac{r^2}{r_a^2} \right) \rho_*(r) \quad (5)$$

is the so-called augmented density (see, e.g., Binney & Tremaine 2008).

In the MOND (and in the ENS) cases a similar formula holds, i.e.

$$f_M(Q) = \frac{1}{\sqrt{8\pi^2}} \frac{d}{dQ} \int_{-\infty}^Q \frac{d\rho_*}{d\Psi} \frac{d\Psi}{\sqrt{Q - \Psi}}, \quad (6)$$

where now Ψ is the MOND relative potential that, by construction, is also the total potential of the ENS. Note that, at variance with equation (4), the lower integration limit is now $-\infty$: due to the far-field logarithmic behaviour of the MOND potential in isolated systems of finite mass, the distribution function must be positive for all values of $Q < 0$ in analogy with finite-mass Newtonian system in a total isothermal potential, where stars of all energies are bound (e.g. Ciotti et al. 2009). Apart from a few exceptions (see Section 3.2.3), in

² Recently an alternative non-relativistic formulation of MOND, dubbed QUMOND, has been proposed (Milgrom 2010).

Table 1. Main properties of the studied families of models.

Family (1)	Gravity (2)	$(M_{\text{DM}}/M_*)_{\text{half}}$ (3)	$r_{\text{ac}}/r_{\text{half}}$ (4)	$r_{\text{as}}/r_{\text{half}}$ (5)	ξ_s (6)	$\xi_{\text{half},s}$ (7)
N_0	Newton	0	0.092	~ 0.8	~ 1.75	~ 1.34
$M_0\kappa_{10}$	MOND	0	0.092	~ 1.0	~ 2.33	~ 1.26
$E_0\kappa_{10}$	Newton	0.76	0.092	~ 0.5	~ 3.48	~ 1.83
$M_0\kappa_{0.01}$	MOND	0	0.092	~ 1.0	~ 2.48	~ 1.28
$E_0\kappa_{0.01}$	Newton	50.1	0.092	< 0.2	> 7.48	> 4.06
N_1	Newton	0	0.053	~ 0.8	~ 1.64	~ 1.28
$M_1\kappa_{10}$	MOND	0	0.053	~ 0.8	~ 2.32	~ 1.31
$E_1\kappa_{10}$	Newton	0.31	0.053	~ 0.6	~ 2.70	~ 1.50
$M_1\kappa_{0.01}$	MOND	0	0.053	~ 0.9	~ 2.61	~ 1.31
$E_1\kappa_{0.01}$	Newton	32.7	0.053	< 0.2	> 6.86	> 3.64

(1) Name of the family of models: N are the Newtonian purely baryonic models, M the MOND models, and E the ENS models. The first subscript is the value of the parameter γ identifying the stellar density profile (equation 2); the second subscript is the value of the internal acceleration ratio $\kappa \equiv GM_*/a_0 r_*^2$. (2) Gravity law. (3) DM-to-stellar mass ratio within the stellar half-mass radius r_{half} ($r_{\text{half}} \simeq 3.84r_*$ for $\gamma = 0$ and $r_{\text{half}} \simeq 2.41r_*$ for $\gamma = 1$). (4) Normalized critical anisotropy radius for consistency, as determined from the GDSAI. Models with $r_a < r_{\text{ac}}$ are necessarily inconsistent. (5) Normalized minimum anisotropy radius for stability. (6) Maximum value for stability of the Fridman-Polyachenko-Shukhman parameter. (7) Maximum value for stability of the radial-to-tangential kinetic energy ratio measured within r_{half} . In the columns (5-7), upper limits on r_a and lower limits on ξ_s and $\xi_{\text{half},s}$ mean that no instability has been detected in the most anisotropic case explored for that family.

the simulations of the ENSs the halo is maintained “frozen” (i.e. it acts as a fixed external potential), so its distribution function is not needed.

2.1 Consistency

As well known, in (single- or multi-component) OM models it is possible to determine a critical value of the anisotropy radius of each density component, r_{ac} , so that for $r_a < r_{\text{ac}}$ the models are inconsistent, i.e., $f(Q) < 0$ for some admissible value of Q . A necessary condition for consistency of OM models is $d\rho_*(r)/dr \leq 0$ at all radii (Ciotti & Pellegrini 1992; Ciotti 1996, 1999; Ciotti et al. 2009). As recently proved in Ciotti & Morganti (2010a,b; see also Van Hese, Baes & Dejonghe 2011; An 2011) this condition is rigorously equivalent to the Global Density Slope-Anisotropy Inequality (GDSAI), i.e. to the requirement that at each radius the negative of the logarithmic slope of the stellar density distribution cannot be less than twice the local value of the anisotropy parameter, $\gamma_*(r) \geq 2\beta(r)$. Remarkably, it is easy to show that the GDSAI is independent of the gravity law holding the system together, so that it holds not only for Newtonian multi-component systems (such as the ENS), but also in the MOND case³.

We applied the GDSAI to our families of models, determining for each stellar density profile the value of r_{ac} (see Table 1), and the obtained limits coincide with those determined in Ciotti (1999). As these are just necessary conditions for consistency, the positivity of the distribution function must still be checked numerically for $r_a \geq r_{\text{ac}}$. We also note that from the inequality $d\rho_*(r)/dr \leq 0$ it follows that in case of isotropy ($r_a = \infty$) a spherical density distribution must be necessarily monotonically decreasing for increasing r , and this imposes quite strong constraints on the DM halos

of physically admissible ENS. If the halo has a central “hole” (which is not unusual for ENSs; see Nipoti et al. 2007c), it can be physically realized only if its orbital distribution is tangentially biased, at least in the internal regions. In practice, this is not an issue in simulations with frozen DM halos, but it is an important problem when setting up initial conditions for simulations in which the DM halo is “live” (i.e. modelled with particles; see Section 3.2.3).

3 STABILITY

We now describe the main results of the N -body simulations. Before, we briefly illustrate the numerical code N-MODY and the tests performed.

3.1 The numerical simulations

We ran N -body simulations with N-MODY, our original parallel three-dimensional particle-mesh code that can be used to follow the evolution of either MOND or Newtonian collisionless stellar systems (Nipoti et al. 2007a; Londrillo & Nipoti 2009). In previous papers we have already used N-MODY to demonstrate significant differences in violent relaxation, merging and dynamical friction in MOND and Newtonian dynamics (Nipoti et al. 2007a,c; Ciotti et al. 2007; Nipoti et al. 2008). We refer the readers to these papers and to Londrillo & Nipoti (2009) for a more detailed description of the code. In the present study the spherical grid has 64 radial nodes, 32 nodes in colatitude ϑ and 64 nodes in azimuth φ , and the total number of particles is $N_{\text{part}} \simeq 8 \times 10^5$. We verified with convergence experiments that these numbers of particles and grid points exclude important discreteness effects. In particular we reran some of the simulations with a grid $128 \times 64 \times 128$ and $N_{\text{part}} \simeq 6.4 \times 10^6$, finding that the results are almost identical to the corresponding lower-resolution cases.

In each simulation the initial conditions consist of an

³ This however is not true for the *sufficient conditions* for consistency (see Ciotti & Morganti 2010a,b)

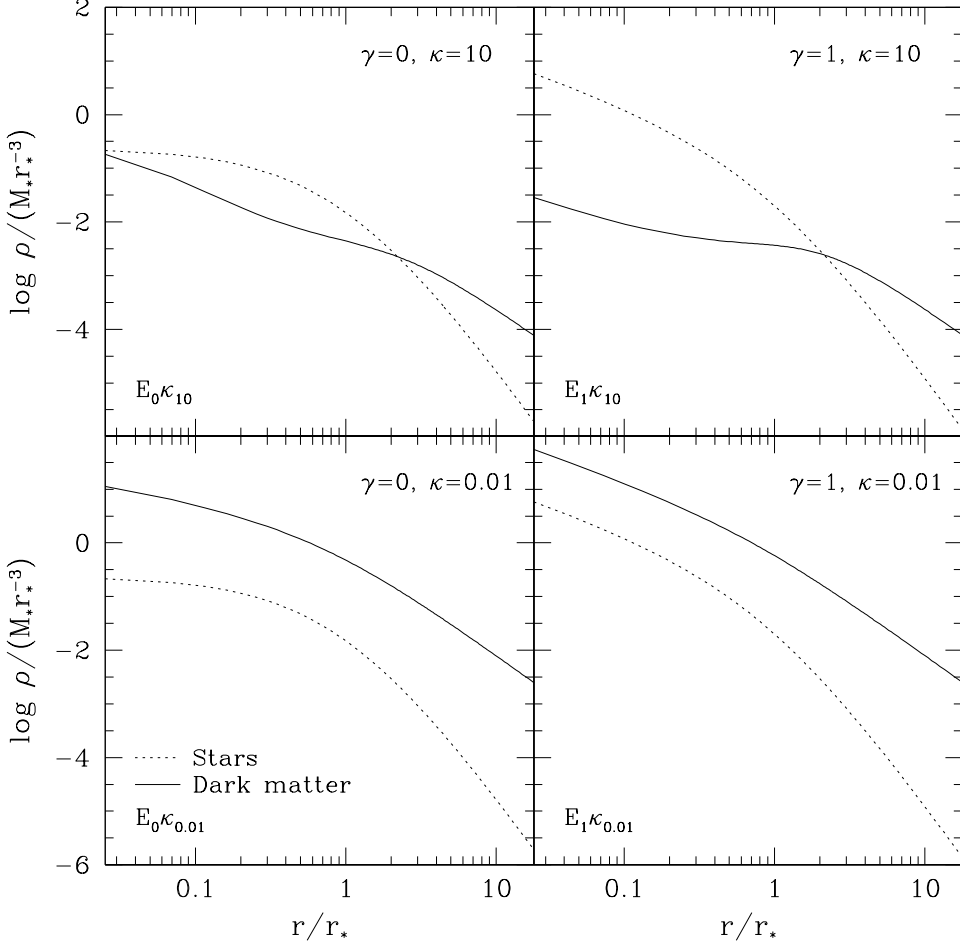


Figure 1. Stellar (dotted curves) and DM (solid curves) density profiles of ENSs corresponding to spherical MOND $\gamma = 0$ (left column) and $\gamma = 1$ (right column) models, for two different values of the dimensionless acceleration ratio $\kappa = GM_*/a_0 r_*^2$.

N -body realization of the stellar distribution of an isolated equilibrium galaxy model, in which the particles are distributed in phase space with the standard rejection technique, using the numerically recovered distribution functions. In the ENS simulations, even if the DM halo is frozen, the systems are truncated exponentially at a radius r_t , so that the potential well is finite. As a rule, we adopt $r_t = 10r_*$, but we ran some of the simulations also with $r_t = 100r_*$ and $r_t = 1000r_*$, finding that the stability properties of a model do not depend on the specific choice of the truncation radius.

Following Nipoti et al. (2007c), we identify each MOND initial condition by fixing a value of the dimensionless internal acceleration parameter $\kappa \equiv GM_*/a_0 r_*^2$, so M_* and r_* are not independent quantities. In physical units, introducing the quantity $M_{*,10} \equiv M_*/10^{10} M_\odot$, $r_* \simeq 3.4\kappa^{-1/2} M_{*,10}^{1/2}$ kpc, the time and velocity units are $t_* \equiv \sqrt{r_*^3/GM_*} \simeq 29.7\kappa^{-3/4} M_{*,10}^{1/4}$ Myr, and $v_* \equiv r_*/t_* \simeq 112\kappa^{1/4} M_{*,10}^{1/4}$ km s $^{-1}$. The simulations are evolved up to $100t_{\text{dyn}}$ with a time step $\Delta t = 0.01t_{\text{dyn}}$, where t_{dyn} is the characteristic dynamical time of the system. In the purely

baryonic Newtonian γ -models, we adopt the standard half-mass radius value

$$t_{\text{dyn}} \equiv \sqrt{\frac{3\pi}{16G\rho_{\text{half}}}} = \frac{\pi t_*}{\sqrt{2}[2^{1/(3-\gamma)} - 1]^{3/2}}, \quad (7)$$

where $\rho_{\text{half}} = 3M_*/8\pi r_{\text{half}}^3$ is the mean stellar density inside the half-mass radius r_{half} (we recall that $r_{\text{half}} \simeq 3.84r_*$ for $\gamma = 0$ and $r_{\text{half}} \simeq 2.41r_*$ for $\gamma = 1$). In the corresponding MOND models (and their ENSs), t_{dyn} is given by the above expression multiplied by v_c^N/v_c^M , where v_c^N is the circular velocity at r_{half} for the purely baryonic Newtonian system and v_c^M is the same quantity for the MOND system.

Following Nipoti et al. (2002), in order to determine whether a given model is unstable, we check its departures from spherical symmetry by monitoring the evolution of its intrinsic axis ratios c/a and b/a (where a , b and c are the longest, intermediate and shortest axes of the inertia ellipsoid of the stellar distribution). As preliminary tests we ran simulations in which the initial conditions are isotropic purely baryonic Newtonian, MOND and ENSs. We found that numerical uncertainties (due to the finite number of particles) on c/a and b/a never exceed 1% over $100t_{\text{dyn}}$ of evolution of these stable isotropic models. As a conse-

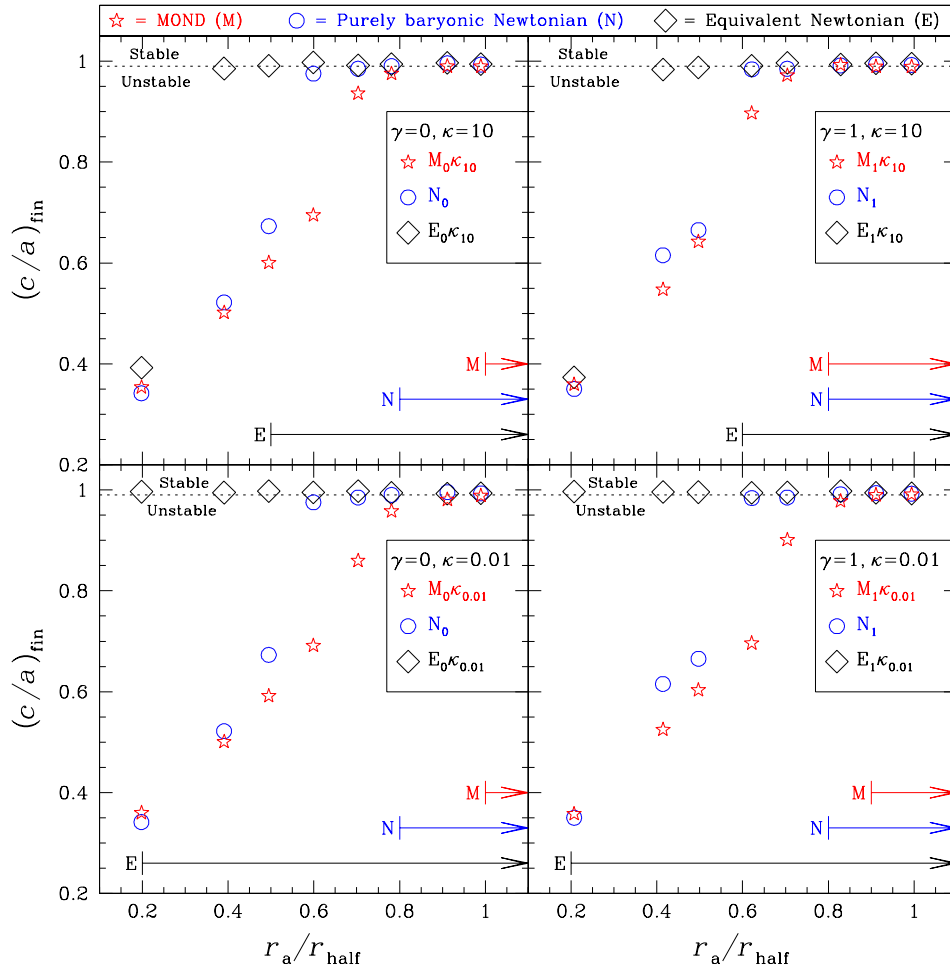


Figure 2. Final axis ratio $(c/a)_{\text{fin}}$ as a function of the initial anisotropy radius normalized to the half-mass radius for MOND (stars), purely baryonic Newtonian (circles), and ENSs (squares) with different values of γ and κ . In each panel the horizontal dashed line marks the fiducial threshold value for stability, $(c/a)_{\text{fin}} = 0.99$; the arrows indicate the range of r_a/r_{half} corresponding to stable models.

quence, we define *unstable* the models for which the axis ratio $(c/a)_{\text{fin}}$ after $100 t_{\text{dyn}}$ is smaller than a fiducial threshold value $c/a = 0.99$. In the simulations the onset of the instability is just due to numerical noise produced by discreteness effects in the initial conditions. As expected, we found that an exact determination of the stability threshold for a given family of models is not straightforward: while for strongly anisotropic initial conditions the onset of the instability is apparent and the numerical models settle down into a final equilibrium configuration in a few dynamical times, for nearly stable initial conditions the instability can be characterized by very slow growth rates and its effects become evident even after tens of t_{dyn} .

3.2 Results

For a given initial stellar density profile (i.e. $\gamma = 0$ or $\gamma = 1$ in equation 2), we explored, besides the purely baryonic Newtonian case (models N_0 and N_1 in Table 1), two families of MOND systems (and the corresponding families of ENSs), characterized by the values of the acceleration ratio $\kappa = 0.01$ and $\kappa = 10$ (see Table 1 for a summary). The cases

with $\kappa = 0.01$ correspond to low-acceleration systems with internal accelerations everywhere much lower than a_0 , in the so-called deep-MOND regime. Their associated ENSs are therefore totally DM dominated systems (Table 1, Column 3). On the other hand, the $\kappa = 10$ cases are systems with relatively high accelerations within r_{half} , corresponding in the Newtonian context to systems dominated by baryons in the central regions and by DM only at $r \gtrsim r_{\text{half}}$ (Table 1, Column 3). The four panels of Fig. 1 show the baryonic and DM initial density profiles of the ENSs corresponding to the $\kappa = 0.01$ and $\kappa = 10$ MOND systems, for the two explored values of γ . As can be seen, the associated DM halos do not show a central hole and so, at least from this point of view, are not unrealistic (see Section 2.1).

3.2.1 Minimum value for stability of the anisotropy radius

For each family of models we have a set of eight simulations, in which the initial conditions differ only in the value of the normalized anisotropy radius r_a/r_{half} . This is apparent in Fig. 2, where we plot the final axis ratio $(c/a)_{\text{fin}}$ vs. the initial value of r_a/r_{half} for all the explored models of

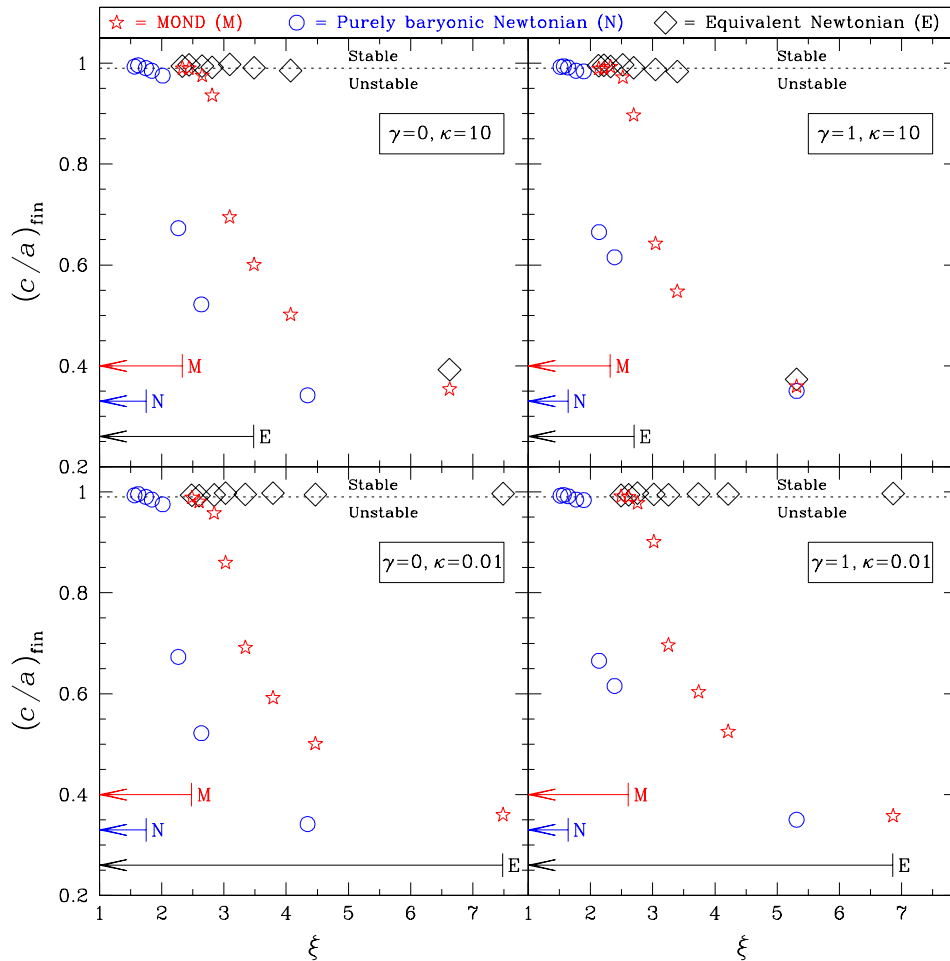


Figure 3. Final axis ratio $(c/a)_{\text{fin}}$ as a function of the Fridman-Polyachenko-Shukhman parameter ξ , for the same models as in Fig. 2. The arrows indicate the range of ξ corresponding to stable models.

the ten families. The stability properties of the models can be inferred directly from Fig. 2: it is clear that the value of r_a at which instability appears is largest for MOND models, smallest for the corresponding ENSs, and intermediate for purely baryonic Newtonian systems. Because of the very nature of the radial-orbit instability (very slow growth rates for marginally unstable systems), a precise determination of the value of the minimum anisotropy radius for stability r_{as} is difficult. What can be estimated robustly with N -body simulations is a fiducial value of r_{as} separating apparently unstable systems from *bona fide* stable systems. Adopting as fiducial threshold for stability $(c/a)_{\text{fin}} = 0.99$ (horizontal dashed line in each panel of Fig. 2), we estimate for each family of models the minimum anisotropy radius for stability r_{as} , which is reported (in units of r_{half}) in Table 1.

As expected, the differences in the stability limit between MOND and ENSs are more evident in systems with lower values of the acceleration ratio κ (or, from a Newtonian point of view, for more DM dominated systems). For instance, if we consider $\gamma = 0$ models with $\kappa = 0.01$, which are representative of low-surface density systems with flat inner stellar density profile (such as dwarf spheroidal galaxies), we find $r_{\text{as}}/r_{\text{half}} \sim 1$ for MOND and $r_{\text{as}}/r_{\text{half}} < 0.2$

for the ENS; very similar results are obtained for the more peaked Hernquist $\gamma = 1$ models. Unsurprisingly, Newtonian models with the DM halo are less subject to the radial-orbit instability than the purely baryonic Newtonian models.

Thus, from this first analysis we conclude that, when using r_a/r_{half} as an indicator of the amount of admissible radial orbits, MOND systems are more prone to radial-orbit instability than their associated ENSs, and also than corresponding purely baryonic Newtonian models. However, as we will see in the next Section, the comparison between the MOND and the associated purely baryonic Newtonian families is subtle: the fact that the latter typically admit smaller r_a/r_{half} values does not imply that (globally) they can sustain more radial kinetic energy.

3.2.2 Maximum value for stability of the ξ parameter

Stability limitations expressed in terms of r_a are particularly relevant to observational works, as r_a enters directly in the Jeans equations that are routinely used to fit the velocity-dispersion profiles of stellar systems. However, from a deeper point of view, the value of r_a (loosely speaking, the radius outside which orbits are mainly radial) is not a ro-

bust measure of the fraction of kinetic energy that is stored in radial orbits, which, at least in the Newtonian context, is believed to be the main indicator of the tendency to develop radial-orbit instability. More specifically, it has been argued (Polyachenko & Shukhman 1981; Fridman & Polyachenko 1984) that a proper criterion for stability for Newtonian self-gravitating systems can be expressed in terms of the global anisotropy parameter $\xi \equiv 2T_r/T_t$, where T_r and $T_t \equiv T_\psi + T_\phi$ are the radial and tangential components of the kinetic energy tensor, respectively. Global isotropy corresponds to a value of the Fridman-Polyachenko-Shukhman parameter $\xi = 1$. Indications exist that there is a critical value ξ_s such that only systems with $\xi \leq \xi_s$ are stable, and it is widely accepted that $\xi_s \approx 1.7 \pm 0.25$, relatively independent of the specific density distribution.

A priori we do not have reasons to expect that ξ can be used as a stability indicator also in MOND. In any case, by definition ξ_s measures how much radial anisotropy can be supported by a stable system, so it is interesting to discuss the stability properties of our MOND, purely baryonic Newtonian and ENSs in terms of ξ . The values of ξ_s for the families of models studied in the present work are reported in Table 1, and in Fig. 3 we show all the models in the $(c/a)_{\text{bn}}-\xi$ plane to be compared with the analogous Fig. 2.

For the purely baryonic Newtonian models the interpretation of these numbers is straightforward: we find $\xi_s \sim 1.6 - 1.8$, in agreement with the standard criterion and with previous numerical studies (see, e.g., Nipoti et al. 2002). For the MOND models we find $2.3 \lesssim \xi_s \lesssim 2.6$, with ξ_s depending on both the stellar density profile and the acceleration ratio κ . These values are substantially higher than those found for the corresponding purely baryonic Newtonian models, indicating that, for given density distribution, MOND systems can sustain more radial kinetic energy than Newtonian systems without DM. This is not in contrast with the findings reported in the previous Section, i.e. that MOND models have larger r_{as} than purely baryonic Newtonian models. In fact, for fixed density profile and r_a value, a MOND model has higher ξ than a purely baryonic Newtonian model, because more kinetic energy is stored in the outer parts, where orbits are radially biased and the gravitational field of MOND systems is stronger⁴. Apparently, this effect compensates the larger values of admissible r_a . Instead, the ENSs are again found able to sustain systematically higher values of ξ_s than the corresponding families MOND systems, and this clearly indicates that MOND systems are more subject to radial-orbit instability than Newtonian models with DM and identical total gravitational field.

In general, for both MOND and ENSs we find a substantial spread in the values of ξ_s , supporting the expectation that a “universal” value of ξ_s does not exist for these systems (for Newtonian models with DM, extended versions of the stability criterion have been proposed; Polyachenko 1987; Stiavelli & Sparke 1991). The data in Table 1 suggest that in MOND, and even more in the ENSs, ξ_s increases (i.e., relatively more kinetic energy can be stored in radial orbits) for decreasing κ . While for the ENSs this trend can be explained because in the limit $\kappa \rightarrow 0$ the stars become

just tracers, it is tempting to speculate that in MOND this behaviour can be interpreted as a manifestation of the less mixing nature of MOND with respect to Newtonian gravity. This interpretation is supported by the well established numerical finding that phase mixing (Ciotti et al. 2007) and violent relaxation (Nipoti et al. 2007a) in MOND systems take longer (in units of dynamical times) than in the Newtonian case. Very qualitatively, the deep-MOND force between particles behaves like $1/r$, i.e. it is nearer to the harmonic oscillator force than the $1/r^2$ force, and it is easy to show that a system in which particles interact with the harmonic oscillator force, no mixing or instabilities are possible, as each particle moves independently of the others (Lynden-Bell & Lynden-Bell 1982). Curiously, even though MOND forces in a system of particles are non-additive, a similar trend towards longer relaxation times has been also found recently in shell models interacting with additive $1/r^\alpha$ forces (Di Cintio & Ciotti 2011), and the phase-space evolution of the case with $1/r$ forces is strikingly similar to the deep-MOND collapses presented in Ciotti et al. (2007).

The fact that ξ in MOND is strongly affected by the properties of the system at large radii suggests to consider as a possible stability indicator the quantity ξ_{half} , defined as the ratio of radial to tangential kinetic energy within r_{half} : the maximum values for stability $\xi_{\text{half},s}$ for our families of models are reported in the last column of Table 1. Remarkably, all our MOND and purely baryonic Newtonian families have $\xi_{\text{half},s} \sim 1.3$, while the ENSs have $\xi_{\text{half},s} \gtrsim 1.5$ (for $\kappa = 10$) and $\xi_{\text{half},s} \gtrsim 3.6$ (for $\kappa = 0.01$), which leads us to speculate that *a limit on the amount of the radial orbits within the half-mass radius might be used as an empirical stability criterion for MOND stellar systems, valid from the Newtonian to the deep-MOND regime, i.e. independent of the value of the internal acceleration relative to a_0* . This result is reminiscent of that of Trenti & Bertin (2006), who found that an almost isotropic core can stabilize Newtonian self-gravitating systems with very strong global radial anisotropy.

3.2.3 Simulations of equivalent Newtonian systems with live dark-matter halos

The results on the stability of the ENSs might be affected to some extent by our assumption of frozen DM halo, because it is possible that an ENS with live DM halo has different stability properties (see Stiavelli & Sparke 1991). In order to assess to what extent our results are affected by the assumption of frozen DM halos, we reran the ENS simulations of the family $E_0\kappa_{10}$ with live DM halos. For technical reasons we ran these live-halo simulations with our FVFPs treecode (Fortran Version of a Fast Poisson Solver; Londrillo, Nipoti, & Ciotti 2003; Nipoti, Londrillo, & Ciotti 2003), which was already tested against N-MODY in Nipoti et al. (2007c). As an additional test, we reran with FVFPs all the purely baryonic Newtonian simulations of the family N_0 , finding excellent agreement with those run with N-MODY. In the live-halo simulations of the models of the family $E_0\kappa_{10}$ we used $\simeq 8 \times 10^5$ particles for the stellar component and $\simeq 1.3 \times 10^6$ particles for the halo, which has mass $\simeq 1.6M_*$ for the adopted truncation radius $r_t = 10r_*$. We verified numerically that for these two-component $E_0\kappa_{10}$ models the halo density distribution, which is monotonically decreasing

⁴ Note that by construction a MOND model and its ENS, with identical value of r_a , have the same value of ξ .

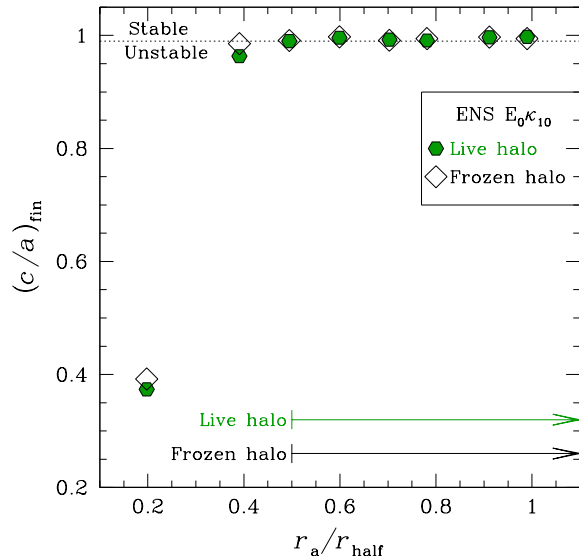


Figure 4. Final axis ratio $(c/a)_{\text{fin}}$ as a function of the initial anisotropy radius normalized to the half-mass radius for the ENSs with $\gamma = 0$ and $\kappa = 10$ when the DM halo is live (hexagons) and frozen (squares). The range of r_a/r_{half} corresponding to stable models (indicated by the arrows) is the same in the two cases.

(see Fig. 1) and thus satisfies the necessary condition for consistency (see Section 2.1), can be generated by a positive isotropic distribution function, which we used to distribute the DM particles in phase space with the standard rejection technique.

The final axis ratios of the live-halo simulations (hexagons in Fig. 4) are not significantly different from those of the corresponding frozen-halo simulations (squares in Fig. 4). It follows that the stability properties of the $E_0\kappa_{10}$ family of models do not depend on whether the halo is modelled with particles or it is a fixed potential: in particular the values of the minimum anisotropy radius r_{as} (and then of the maximum Fridman-Polyachenko-Shukhman parameter ξ_s) for stability are the same in the two cases. These results suggest that our conclusion that MOND models are substantially more subject to radial-orbit instability than ENSs should be robust, at least if the DM halos are almost isotropic. Though the assumption of isotropy of the halos is not necessarily justified, given that the anisotropy of DM distributions is hard to constrain, it is clear that an isotropic halo can be always be invoked, in the context of Newtonian gravity, to stabilize an otherwise unstable strongly radially-anisotropic stellar system, while this freedom is not allowed in the context of MOND.

4 DISCUSSION AND CONCLUSIONS

To some extent, the MOND and DM interpretations of the kinematics of galaxies can be considered degenerate, i.e. several observational features can be satisfactorily reproduced in both paradigms. This raises interesting questions about possible tests to discriminate between MOND and Newtonian gravity with DM. Fortunately, it is now well established

that some important dynamical processes *are* different, even in systems in which the total gravitational potentials are identical. Examples are dynamical friction and two-body relaxation.

In the present work we explored whether radial-orbit instability acts differently in MOND and in Newtonian gravity (with and without DM); in addition to the theoretical interest, this study can be useful to constrain the interpretation of the observed kinematics of stellar systems in the two cases. In particular, we have focused on the stability of OM radially-anisotropic spherical γ -models ($\gamma = 0$ and $\gamma = 1$). We compared the results obtained for MOND models, ENSs and purely baryonic Newtonian systems, all with the same stellar density distribution. Overall, we found that MOND systems are more prone to radial-orbit instability than their ENSs, independent of the specific indicator (r_a or ξ) used to quantify the anisotropy. Compared to purely baryonic Newtonian systems with the same density profile, however, MOND systems have larger minimum anisotropy radius for stability r_{as} , but nevertheless higher maximum global anisotropy parameter for stability ξ_s , a consequence of the larger kinetic energy that can be stored in their outer regions. We speculate that ξ_s is larger in MOND systems than in Newtonian systems with no DM for the same reasons that phase mixing and violent relaxation are less efficient, i.e., because the force between particles in deep-MOND decreases with distance less strongly (qualitatively as $1/r$) than in Newtonian gravity, so being nearer to the special case of harmonic oscillator inter-particle forces, when instabilities and energy exchanges are impossible.

Observationally, these findings may be relevant to applications of MOND to pressure-supported systems such as globular clusters, dwarf spheroidal and elliptical galaxies. For instance, the velocity-dispersion profiles of globular clusters in the outer parts of the Milky Way can be used to test MOND. In the case of the globular cluster NGC 2419 strong OM radial anisotropy (r_a close to r_{ac}) might be required in order to bring the velocity dispersion profile predicted by MOND close to the profile inferred from the observed radial velocities of the cluster stars (Sollima & Nipoti 2010). A combination of the stability constraints discussed in this paper with new observations of the radial velocity of stars can make the kinematics of NGC 2419 a crucial test for MOND (Ibata et al., in preparation).

Another family of objects that are very interesting from the perspective of MOND is that of dwarf spheroidal galaxies, because their low surface-brightness, combined with their measured velocity dispersion, lead to conclude that they must be DM dominated if Newtonian gravity holds. Angus (2008) studied the observed line-of-sight velocity-dispersion profiles of Milky Way dwarf spheroidal galaxies, finding that in most cases the data can be reproduced in MOND, at least with somewhat *ad hoc* anisotropy profiles. This result should be reconsidered on the basis of the consistency and stability constraints discussed in the present work.

The kinematics of elliptical galaxies has also been considered as a possible test for MOND (e.g. Sanders 2000). As for globular clusters and dwarf spheroidals, when trying to reproduce the kinematics of ellipticals, the anisotropy of the velocity distribution of the stars is one of the variables in the problem and it is important to constrain it as much as

possible, along the lines described in the present paper. For instance, consistency constraints (but not the more stringent stability constraints) on the anisotropy of stars are considered in the recent investigation by Cardone et al. (2010). Some authors (Tiret et al. 2007; Klypin & Prada 2009) used the observed kinematics of planetary nebulae or of the satellites around elliptical galaxies as a test for MOND, allowing for quite general anisotropy profiles for the satellite system. In this case, however, while some limits on the amount of radial anisotropy might come from the requirement of consistency, stability arguments do not necessarily lead to strong constraints as long as the considered tracers are not dynamical dominant.

ACKNOWLEDGEMENTS

Most numerical simulations were performed at CINECA, Bologna, with CPU time assigned under the INAF-CINECA agreement 2008/2010. L.C. and C.N. are supported by the MIUR grant PRIN2008.

REFERENCES

- An J., 2011, arXiv:1101.0006
 An J.H., Evans N.W., 2006, ApJ, 642, 752
 Angus G. W., 2008, MNRAS, 387, 1481
 Barnes J., Hut P., Goodman J., 1986, ApJ, 300, 112
 Barnes E. I., Lanzel P. A., Williams L. L. R., 2009, ApJ, 704, 372
 Bekenstein J. D., Milgrom M., 1984, ApJ, 286, 7
 Bertin G., Pegoraro F., Rubini F., Vesperini E., 1994, ApJ, 434, 94
 Binney J., Tremaine S., 2008, Galactic Dynamics 2nd Ed., Princeton University Press, Princeton
 Brada R., Milgrom M., 1999, ApJ, 519, 590
 Cardone V. F., Angus G., Diaferio A., Tortora C., Molinaro R., 2010, arXiv:1011.574
 Christodoulou D. M., 1991, ApJ, 372, 471
 Ciotti L., 1996, ApJ, 471, 68
 Ciotti L., 1999, ApJ, 520, 574
 Ciotti L., Binney J., 2004, MNRAS, 351, 285
 Ciotti L., Morganti L., 2009, MNRAS, 393, 179
 Ciotti L., Morganti L., 2010a, MNRAS, 401, 1091
 Ciotti L., Morganti L., 2010b, MNRAS, 408, 1070
 Ciotti L., Pellegrini S., 1992, MNRAS, 255, 561
 Ciotti L., Londrillo P., Nipoti C., 2006, ApJ, 640, 741
 Ciotti L., Nipoti C., Londrillo P., 2007, in Collective Phenomena in Macroscopic Systems, ed. G. Bertin et al. (Singapore: World Scientific), p.177
 Ciotti L., Morganti L., de Zeeuw P. T., 2009, MNRAS, 393, 491
 Dehnen, W. 1993, MNRAS, 265, 250
 Dejonghe H., Merritt D., 1988, ApJ, 328, 93
 Di Cintio P., Ciotti L., 2011, submitted
 Fridman A. M., Polyachenko V. L., 1984, Physics of Gravitating Systems. Springer, New York
 Henon M., 1973, A&A, 24, 229
 Hernquist L., 1990, ApJ, 356, 359
 Hjorth J., 1994, ApJ, 424, 106
 Klypin A., Prada F., 2009, ApJ, 690, 1488
 Londrillo P., Nipoti C., Ciotti L., 2003, MSAIS, 1, 18
 Londrillo P., Nipoti C., 2009, MSAIS, 13, 89
 May A., Binney J., 1986, MNRAS, 221, 13P
 Lynden-Bell D., Lynden-Bell R. M., 1982, Proceedings: Mathematical, Physical and Engineering Sciences, Vol. 455, No. 1982, p. 475, The Royal Society
 Merritt, D. 1985, AJ, 90, 102
 Merritt D., Aguilar L. A., 1985, MNRAS, 217, 787
 Meza A., Zamorano N., 1997, ApJ, 490, 136
 Meza A., Zamorano N., 1998, ASPC, 136, 400
 Milgrom M., 1983, ApJ, 270, 365
 Milgrom M., 1986, ApJ, 306, 9
 Milgrom M., 1989, ApJ, 338, 121
 Milgrom M., 2001, MNRAS, 326, 1261
 Milgrom M., 2010, MNRAS, 403, 886
 Nipoti C., Londrillo P., Ciotti L., 2002, MNRAS, 332, 901
 Nipoti C., Londrillo P., Ciotti L., 2003, MNRAS, 342, 501
 Nipoti C., Londrillo P., Ciotti L., 2007a, ApJ, 660, 256
 Nipoti C., Londrillo P., Zhao H.S., Ciotti L., 2007b, MNRAS, 379, 597
 Nipoti C., Londrillo P., Ciotti L., 2007c, MNRAS, 381, L104
 Nipoti C., Ciotti L., Binney J., Londrillo P., 2008, MNRAS, 386, 2194
 Osipkov, L.P. 1979, Soviet Astron. Lett., 5, 42
 Ostriker J. P., Peebles P. J. E., 1973, ApJ, 186, 467
 Palmer P. L., Papaloizou J., 1987, MNRAS, 224, 1043
 Polyachenko V. L., 1987, IAUS, 127, 301
 Polyachenko V. L., Shukhman I. G., 1981, SvA, 25, 533
 Saha P., 1991, MNRAS, 248, 494
 Sanders R. H., 2000, MNRAS, 313, 767
 Sanders R. H., McGaugh S. S., 2002, ARA&A, 40, 263
 Sanders R. H., Noordermeer E., 2007, MNRAS, 379, 702
 Sollima A., Nipoti C., 2010, MNRAS, 401, 131
 Stiavelli M., Sparke L. S., 1991, ApJ, 382, 466
 Swaters R. A., Sanders R. H., McGaugh S. S., 2010, ApJ, 718, 380
 Tiret O., Combes F., 2007, A&A, 464, 517
 Tiret O., Combes F., Angus G. W., Famaey B., Zhao H. S., 2007, A&A, 476, L1
 Tremaine S., Richstone D. O., Byun Y.-I., Dressler A., Faber S. M., Grillmair C., Kormendy J., Lauer T. R., 1994, AJ, 107, 634
 Trenti M., Bertin G., 2006, ApJ, 637, 717
 Van Hese E., Baes M., Dejonghe H., 2011, ApJ, 726, 80
 Weinberg M. D., 1991, ApJ, 368, 66